

Bayesian Structural Model Updating with Multimodal Variational Autoencoder

Tatsuya Itoi ^{a,*}, Kazuho Amishiki ^b, Sangwon Lee ^a, Taro Yaoyama ^a

^a School of Engineering, The University of Tokyo, 7-3-1 Hongo, Bunkyo-ku, Tokyo, 1138656, Japan

^b Faculty of Engineering, The University of Tokyo, 7-3-1 Hongo, Bunkyo-ku, Tokyo, 1138656, Japan

* Corresponding author.

E-mail address: itoi@g.ecc.u-tokyo.ac.jp (T. Itoi).

keywords: Bayesian model updating, Multimodal variational autoencoder, Structural reliability

ABSTRACT

This paper presents a novel framework for Bayesian structural model updating and proposes a method that utilizes the surrogate unimodal encoders of a multimodal variational autoencoder. This method facilitates an efficient nonparametric estimation of the likelihood describing the observed data. It is particularly suitable for high-dimensional correlated simultaneous observations applicable to various dynamic analysis models. The proposed approach is benchmarked using a numerical model of a single-story frame building with acceleration and dynamic strain measurements.

1. Introduction

The monitoring of civil structures, including buildings, using vibrational responses has gained attention for decades. Methodologies for updating the parameters of dynamic analysis model have been proposed for the condition and performance assessment of a structure using monitoring data. The dynamic analysis model, which is originally based on assumptions made during the design phase, requires adjustments to incorporate monitoring data. These adjustments are crucial for the performance assessment of structures during their lifetimes. Nevertheless, monitoring data such as vibration responses often do not provide sufficient information regarding the parameters of a dynamic analysis model [1], [2]. For instance, vibrational responses during minor earthquakes may not provide information regarding the parameters related to nonlinear responses. Additionally, acceleration monitoring at the floor level does not provide direct information regarding the damage caused to structural or nonstructural members. This lack of information introduces uncertainty in the estimation of model parameters. Consequently, structural model updating techniques should account for such a lack of information and the associated uncertainties in the estimated model parameters. This

can be achieved by describing such uncertainty by a probability distribution of model parameters, or by a family of plausible model parameters when it is numerically estimated, instead of searching for the best estimate [3], [4], [5]. To conduct an effective performance assessment of structures without introducing bias [6], [7], it is essential to have a probability distribution of model parameters for a dynamic analysis model that incorporates these uncertainties. The Bayesian approach is effective for this purpose.

Within the realm of the Bayesian approach, modal-based approaches for Bayesian model updating have been developed [8], [9] [10] [11]. These methods utilize modal parameters such as modal frequencies and mode shapes, estimated from the observed structural responses for model updating. Time-domain approaches [12], [13], [14], which are suitable for situations where the structural properties vary over time, and frequency-domain approaches [15], [16], where both the input and output need to be measured, have also been proposed. Furthermore, methods incorporating machine learning techniques within the Bayesian updating framework such as the active learning of Kriging,[17] a pattern-recognition method [18] and the Bayesian inference approach [19], have been proposed. However, these methods frequently involve approximations and simplifications primarily because of their theoretical limitations. This is particularly true when high-dimensional and correlated observations such as time- or frequency domain data are applied to Bayesian structural model updating [20], [21].

In this study, a versatile framework for Bayesian structural model updating is proposed by employing a multimodal variational autoencoder (VAE) [22], [23], [24]. A multimodal VAE is an enhanced version of the original VAE [25], a notable tool in the fields of machine learning. The proposed methodology provides a robust and efficient means for various structural models and measurements, effectively addressing uncertainties in the updated model parameters. A numerical example is presented as a benchmark for the proposed method, demonstrating the update of the model parameters of a single-story frame building structure equipped with acceleration and dynamic strain measurements.

2. Bayesian model updating with multimodal VAE

2.1 Overview of multimodal VAE

The VAE is a generative model initially proposed by Kingma and Welling [25] and represents both generative and inference models. A graphical model representation of a VAE is illustrated in Fig. 1. The VAE facilitates the inference of latent representations and enables the generation of original data using neural networks.

Consider data $\mathbf{x}_k \in \mathbb{R}^M$ ($k = 1, \dots, N_x$), a column vector with M entries, and the collection of various data simultaneously obtained at different N_x points, $\mathbf{X} = [\mathbf{x}_1 \ \mathbf{x}_2 \ \dots \ \mathbf{x}_{N_x}] \in \mathbb{R}^{M \times N_x}$. \mathbf{x}_k is a typically high dimensional, correlated simultaneous observed data. When the VAE is trained in the space of the structural analysis model, data \mathbf{X} represents multiple outputs from a single response analysis. In VAE, each data \mathbf{X} can be

reconstructed, or transformed, from a N_z dimensional random variable $\mathbf{z} \in \mathbb{R}^{N_z}$ via the generative model, known as the decoder. The solid line in Fig. 1 is a graphical model representation of the decoder. Variable \mathbf{z} is referred to as latent variable. The dimensions of \mathbf{z} , N_z , is usually smaller than the number of elements in \mathbf{X}_k , $N_x \times M$. A sample of \mathbf{X} , denoted as $\mathbf{X}^{(k)}$ ($k = 1, \dots, N$), is generated following the probability distribution $p(\mathbf{X}|\mathbf{z})$, using a sample of \mathbf{z} , denoted as $\mathbf{z}^{(k)}$ ($k = 1, \dots, N$), which follows the probability distribution $p(\mathbf{z})$. The learning of VAE is conducted to minimize the Kullback-Leibler distance between the probability distributions of a random variable \mathbf{z} and the standard normal distribution. Minimization ensures that the probability distribution of \mathbf{z} , where each element is independent of the others, closely approximates the standard normal distribution. Hereafter, $p(\mathbf{z})$ is approximated to be the probability density function of a normal distribution with a mean $\mathbf{0}$ and covariance \mathbf{I} , $N(\mathbf{0}, \mathbf{I})$.

Then, the inverse of the generative model, that is the posterior distribution of \mathbf{z} , $p(\mathbf{z}|\mathbf{X})$, is expressed as follows:

$$p(\mathbf{z}|\mathbf{X}) = \frac{p(\mathbf{X}|\mathbf{z})p(\mathbf{z})}{\int p(\mathbf{X}|\mathbf{z})p(\mathbf{z})d\mathbf{z}} \quad (1)$$

This corresponds to the inference of latent variable \mathbf{z} hidden behind data \mathbf{X} . The dashed line in Fig. 1 denotes the graphical model representation of the inference model $q_\phi(\mathbf{z}|\mathbf{X})$, known as the encoder, which is the approximation of the posterior distribution of \mathbf{z} , i.e., $p(\mathbf{z}|\mathbf{X})$. The decoder and encoder of VAE are modeled using neural networks. Φ denotes the parameters related to the neural network of the encoder.

The objective function $\mathcal{L}(\mathbf{X})$, which is the opposite sign of the loss function, for training the VAE is as follows:

$$\mathcal{L}(\mathbf{X}) = \mathbb{E}_{q_\phi(\mathbf{z}|\mathbf{X})}[\log p(\mathbf{X}|\mathbf{z})] - D_{\text{KL}}[q_\phi(\mathbf{z}|\mathbf{X})||p(\mathbf{z})] \quad (2)$$

where, $\mathbb{E}_{q_\phi(\mathbf{z}|\mathbf{X})}[\blacksquare]$ is the expectation operator with respect to $q_\phi(\mathbf{z}|\mathbf{X})$, and $D_{\text{KL}}[q_\phi(\mathbf{z}|\mathbf{X})||p(\mathbf{z})]$ is Kullback-Leibler distance of $q_\phi(\mathbf{z}|\mathbf{X})$ from $p(\mathbf{z})$. The first term on the right side of Eq. (2) corresponds to the reconstruction term of the decoder and the second term corresponds to the regularization term.

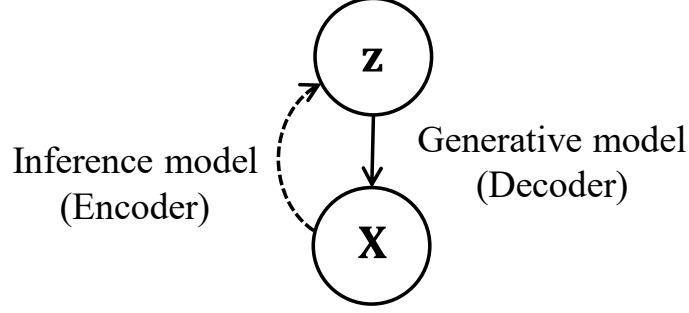


Fig. 1 Graphical model representation of VAE

Multimodal VAE is an enhanced version of the original VAE. The joint multimodal VAE (JMVAE) is a type of multimodal VAE classified as a joint VAE [22]. In the JMVAE-kl proposed by Suzuki et al. [23], [24], a joint VAE capable of learning from multiple modalities with different dimensions is realized by introducing surrogate unimodal encoders, each of which is a VAE for a single modality, in addition to a joint model, as shown in Fig. 2 (a). The dashed lines in Fig. 2 (a) indicate that learning was conducted to minimize the Kullback-Leibler distance between the probability distributions of the outputs from the encoders of the unimodal and joint models, leading to a nearly identical output \mathbf{z} . The objective function for training JMVAE-kl is as follows:

$$\begin{aligned} \mathcal{L}_2(\boldsymbol{\theta}, \mathbf{X}) = & \mathcal{L}_1(\boldsymbol{\theta}, \mathbf{X}) - D_{\text{KL}}[q_{\phi_{\boldsymbol{\theta}}}(\mathbf{z}|\boldsymbol{\theta})||p(\mathbf{z}|\boldsymbol{\theta}, \mathbf{X})] \\ & - D_{\text{KL}}[q_{\phi_{\mathbf{X}}}(\mathbf{z}|\mathbf{X})||p(\mathbf{z}|\boldsymbol{\theta}, \mathbf{X})] \end{aligned} \quad (3)$$

$\mathcal{L}_1(\boldsymbol{\theta}, \mathbf{X})$ in the right-hand side of Eq. (3) can be expressed similarly to Eq. (2) as follows:

$$\mathcal{L}_1(\boldsymbol{\theta}, \mathbf{X}) = \mathbb{E}_{q_{\phi}(\mathbf{z}|\boldsymbol{\theta}, \mathbf{X})}[\log p(\boldsymbol{\theta}, \mathbf{X}|\mathbf{z})] - D_{\text{KL}}[q_{\phi}(\mathbf{z}|\boldsymbol{\theta}, \mathbf{X})||p(\mathbf{z})] \quad (4)$$

where, the first term on the right side of Eq. (4) corresponds to the reconstruction term of the decoder (Fig. 2 (b)) and the second term corresponds to the regularization term.

The use of JMVAE-kl allows for bidirectional generation between modalities. Consider that JMVAE-kl is trained in the space of the dynamic analysis model \mathcal{M} , using the results of the response analyses. Then, the model parameters $\boldsymbol{\theta}$ and their corresponding responses \mathbf{X} are regarded as multiple modalities, which can be generated from each other through a shared representation of latent variables \mathbf{z} .

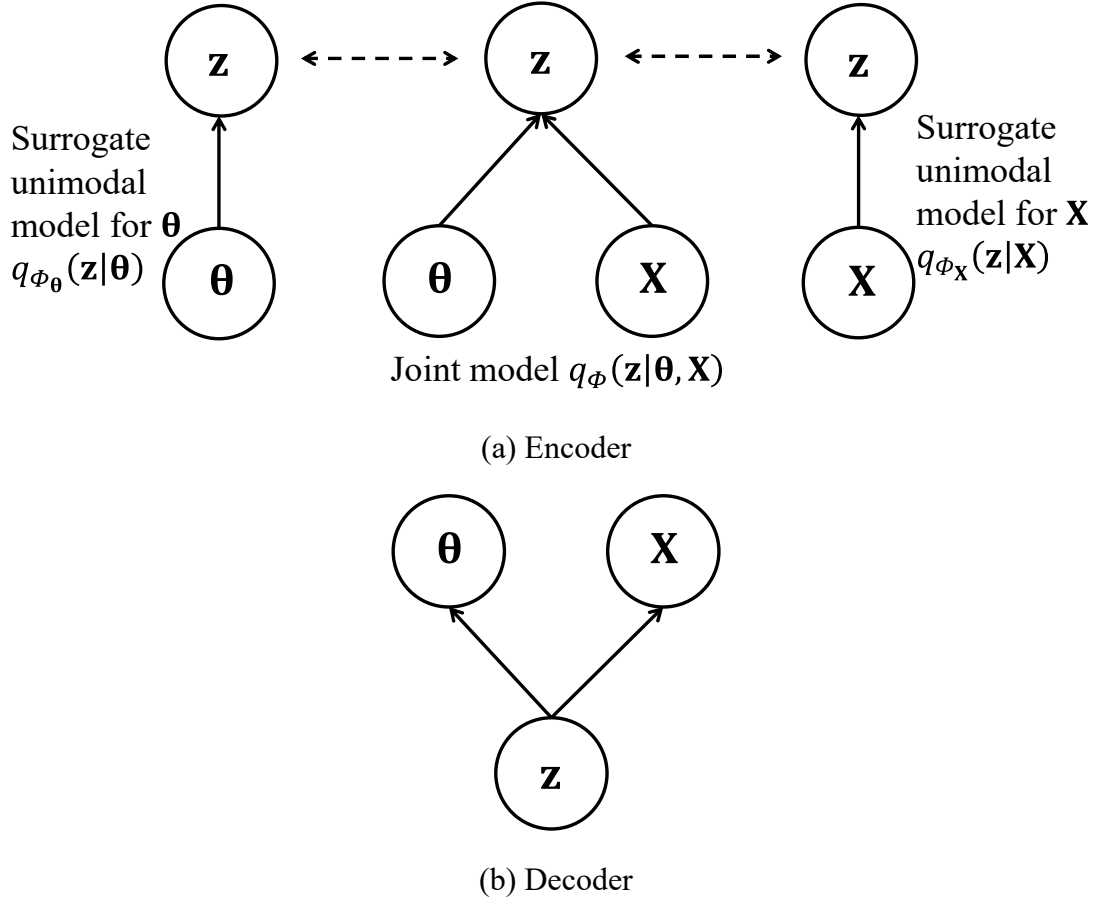


Fig. 2 Graphical model representation of JMVAE-kl

2.2 Likelihood estimation using multimodal VAE

Using Bayes' theorem, the updated probability distribution of the model parameters θ based on the observation \mathbf{X}_{obs} , $p(\theta|\mathbf{X}_{\text{obs}})$, is obtained as follows [5]:

$$p(\theta|\mathbf{X}_{\text{obs}}) = c_1 p(\mathbf{X}_{\text{obs}}|\theta) p(\theta) \quad (5)$$

where, $p(\theta)$ is the prior probability distribution of the model parameters θ . $p(\mathbf{X}_{\text{obs}}|\theta)$ is the probability of obtaining observed data \mathbf{X}_{obs} given the model parameters θ , known as the likelihood function. $c_1 = 1/p(\mathbf{X}_{\text{obs}})$ is the normalizing constant.

By introducing the latent variable \mathbf{z} of VAE [20], the likelihood $(\mathbf{X}_{\text{obs}}|\theta)$ as seen on the right side of Eq. (5) is transformed as follows:

$$p(\mathbf{X}_{\text{obs}}|\theta) = \int p(\mathbf{X}_{\text{obs}}|\mathbf{z}) p(\mathbf{z}|\theta) d\mathbf{z} \quad (6)$$

By applying Bayes' theorem again, the term $p(\mathbf{X}_{\text{obs}}|\mathbf{z})$ on the right-hand side of Eq. (6) can be expressed as follows:

$$p(\mathbf{X}_{\text{obs}}|\mathbf{z}) = \frac{p(\mathbf{z}|\mathbf{X}_{\text{obs}})p(\mathbf{X}_{\text{obs}})}{p(\mathbf{z})} = c_2 \cdot \frac{p(\mathbf{z}|\mathbf{X}_{\text{obs}})}{p(\mathbf{z})} \quad (7)$$

where, c_2 is a normalizing constant. Substituting Eq. (7) into Eq. (6) yields:

$$p(\mathbf{X}_{\text{obs}}|\boldsymbol{\theta}) = c_2 \int_{-\infty}^{\infty} \frac{p(\mathbf{z}|\mathbf{X}_{\text{obs}})p(\mathbf{z}|\boldsymbol{\theta})}{p(\mathbf{z})} d\mathbf{z} \quad (8)$$

In this study, we propose the use of multimodal VAE for the estimation of likelihood $p(\mathbf{X}_{\text{obs}}|\boldsymbol{\theta})$. The framework of the proposed structural model update procedure is illustrated in Fig. 3. As introduced in Section 2.1, the use of surrogate unimodal encoders for $\boldsymbol{\theta}$ and \mathbf{X} in JMVAE-kl, which is trained in the space of the response analyses, enables approximation of $p(\mathbf{z}|\mathbf{X}_{\text{obs}})$ and $p(\mathbf{z}|\boldsymbol{\theta})$. The approximation for $p(\mathbf{z}|\mathbf{X}_{\text{obs}})$ in Eq. (8) is obtained using the surrogate unimodal encoder of \mathbf{X} , $q_{\phi_{\mathbf{X}}}(\mathbf{z}|\mathbf{X})$, by substituting \mathbf{X}_{obs} into $q_{\phi_{\mathbf{X}}}(\mathbf{z}|\mathbf{X})$. The approximation of $p(\mathbf{z}|\boldsymbol{\theta})$ in Eq. (8) is obtained using the surrogate unimodal encoder of $\boldsymbol{\theta}$, $q_{\phi_{\boldsymbol{\theta}}}(\mathbf{z}|\boldsymbol{\theta})$. Notably, when training the VAE, dataset needs to be compiled such that the parameters $\boldsymbol{\theta}$ of the sample response analysis models is uniformly distributed. The computation time needed for calculating the likelihood $p(\mathbf{X}_{\text{obs}}|\boldsymbol{\theta})$ includes the time needed to create the training data and to train the VAE. The calculation of the likelihood itself does not require significant additional time, as it is based on the already trained VAE.

3. Fundamental benchmark for the proposed method

3.1 Problem description

The performance of the proposed method for estimating the likelihood **was** benchmarked using an example problem, as shown in Fig. 3. In this benchmark problem, it was assumed that earthquake monitoring was performed in a target building by observing both input ground motion \mathbf{y}_{obs} and the associated responses \mathbf{X}_{obs} (explained in more detail in Section 3.2). Then, a dataset of responses \mathbf{X} corresponding to the model parameters $\boldsymbol{\theta}$ for training the JMVAE-kl was compiled through a series of response analyses, utilizing the observed input ground motion \mathbf{y}_{obs} as an input (explained in more detail in Section 3.3). Finally, the family of plausible model parameters $\boldsymbol{\theta}$ that effectively reproduces the observed response \mathbf{X}_{obs} was identified, by estimating the likelihood $p(\mathbf{X}_{\text{obs}}|\boldsymbol{\theta})$ using Eq. (8) and the posterior distribution $p(\boldsymbol{\theta}|\mathbf{X}_{\text{obs}})$ using Eq. (4). To calculate the likelihood $p(\mathbf{X}_{\text{obs}}|\boldsymbol{\theta})$, surrogate unimodal encoders both for \mathbf{X} and $\boldsymbol{\theta}$ of JMVAE-kl, $q_{\phi_{\mathbf{X}}}(\mathbf{z}|\mathbf{X})$ and $q_{\phi_{\boldsymbol{\theta}}}(\mathbf{z}|\boldsymbol{\theta})$, were used, as discussed in Section 2 (explained in more detail in Section 3.4).

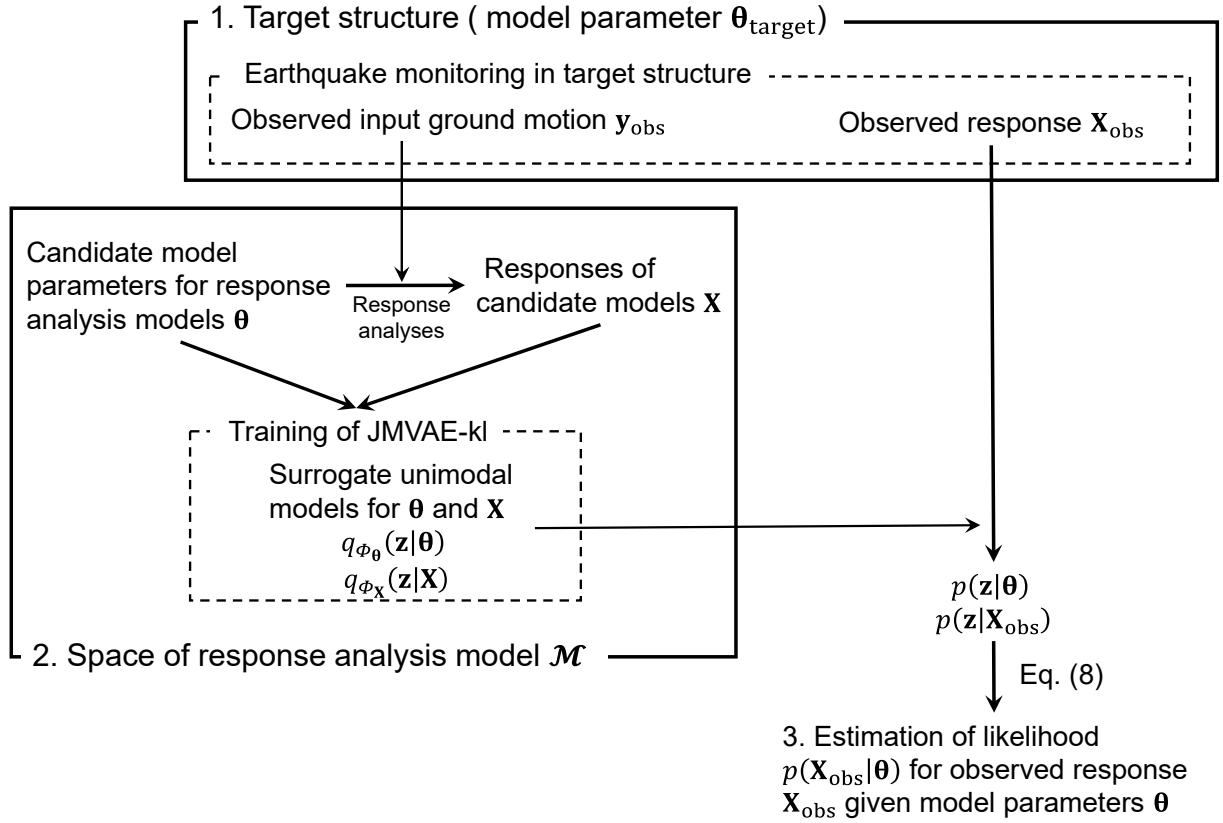


Fig. 3 Framework of the proposed structural model updating procedure for fundamental benchmark problem

3.2 Model description

The simplified frame model shown in Fig. 4 was used as the response analysis model. This model is a plane moment-resisting frame model with rotational springs at the bottom of the columns. The two columns, each with upper and lower part with different sections are connected by a beam to a roof deck. The cross-sectional area, A , the second moment of area, I , of all elements, and the section modulus, Z , of the column members are assumed as shown in Fig. 4. The response analysis was conducted based on OpenSees [26], an open-source software for structural analysis, using its wrapper for Python, OpenSeesPy [27]. This model is based on the real-scale, single-span, single-story building structure presented by Yaoyama et al. [28]. Table 1 lists the target model parameters for the four different cases. The variation in the rotational springs represents damage to the anchor bolts connecting the base plate to the foundation. The mass of the frame structure and roof deck was assumed to be 7000 kg, which was allocated to Nodes 3 and 4. The damping ratio was 0.02 for the first mode and is proportional to the stiffness. In this example, the rotational stiffness of each rotational spring was assumed to be unknown. The effect of the roof deck on the beam was modeled as an increase in the bending stiffness and was also assumed to be unknown. The equivalent bending stiffness $(EI)_{\text{eq}}$, considering the effect of the roof deck, was modeled as follows:

$$(EI)_{eq} = R \cdot (EI)_b \quad (9)$$

where, $(EI)_b$ represents the bending stiffness of the beam, and R is a constant that models the increase in bending stiffness owing to the deck. For the sake of simplicity, the effect of the roof deck on the axial stiffness of the beam was not considered. The other parameters related to the dynamic analysis model were assumed to be known.

In this real-scale structure [28], acceleration measurements are conducted at the basement and roof, whereas dynamic strain measurements are performed on all the columns. The model assumes similar measurement conditions: acceleration measurement at Node 4, dynamic strain measurements at the bottom of Elements 1 and 2, and at the top of Elements 3 and 4. Dynamic strain $\varepsilon_l(t)$ ($l = 1, \dots, 4$) at the location l , which eliminates the effect of axial stress and corresponds to the bending moment, is calculated from the results of response analysis as follows:

$$\varepsilon_l(t) = \frac{M_l(t)}{EZ} \quad (10)$$

where, $M_l(t)$ represents the time history of the bending moment at each location, E is Young's modulus of the steel (205 GPa), and Z_l is the elastic section modulus of each column.

For the input ground motion, the El-Centro acceleration time history record from the 1940 Imperial Valley earthquake (north-south component) was used, with a sampling frequency of 50 Hz and duration of 40.96 seconds, as shown in Fig. 5. The acceleration time histories at Node 4, along with the dynamic strain time histories at the bottom of Elements 1 and 2, and the top of Elements 3 and 4, are stored as responses, as shown in Fig. 6. Gaussian noise with an S/N ratio of 40 dB was added to both the input acceleration and response time histories. The acceleration and dynamic strains exhibited similar temporal characteristics, and the amplitudes of the dynamic strains varied between observation points depending on the conditions of rotational stiffness. The Fourier amplitude spectral ratios of the response to the input acceleration are then obtained, as shown in Fig. 7. Hereafter, the logarithm of these Fourier amplitude spectral ratios from 0.12 to 12.6 Hz, comprising 512 data points, were used as \mathbf{X}_{obs} . The size of \mathbf{X}_{obs} was 5×512 . The design of the measurement and types of data used for the model updating \mathbf{X}_{obs} were variable, which affected the posterior distribution of the model parameters $\boldsymbol{\theta}$, $p(\boldsymbol{\theta}|\mathbf{X}_{obs})$. The optimization of these choices were a topic that warrants further investigation.

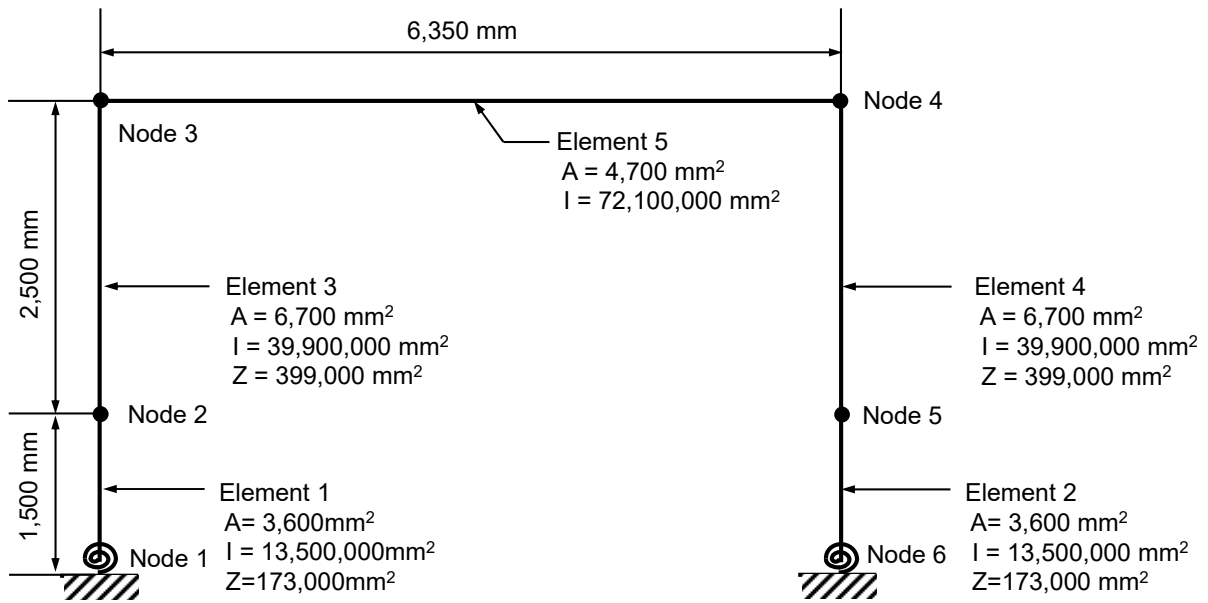


Fig. 4 Flame structure model

Table 1 Target model

	Ratio of $(EI)_{eq}$ to $(EI)_b$	Stiffness of rotational spring at Node 1 [kNm/rad]	Stiffness of rotational spring at Node 6 [kNm/rad]
Case 1	2.0	1000	1000
Case 2	2.0	1000	5000
Case 3	2.0	5000	1000
Case 4	2.0	5000	5000

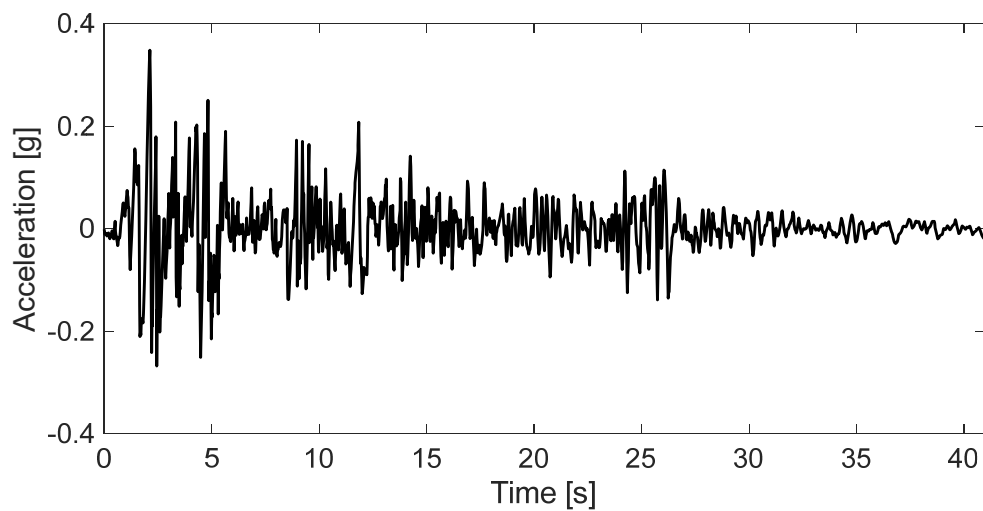


Fig. 5 Acceleration time history of input ground motion

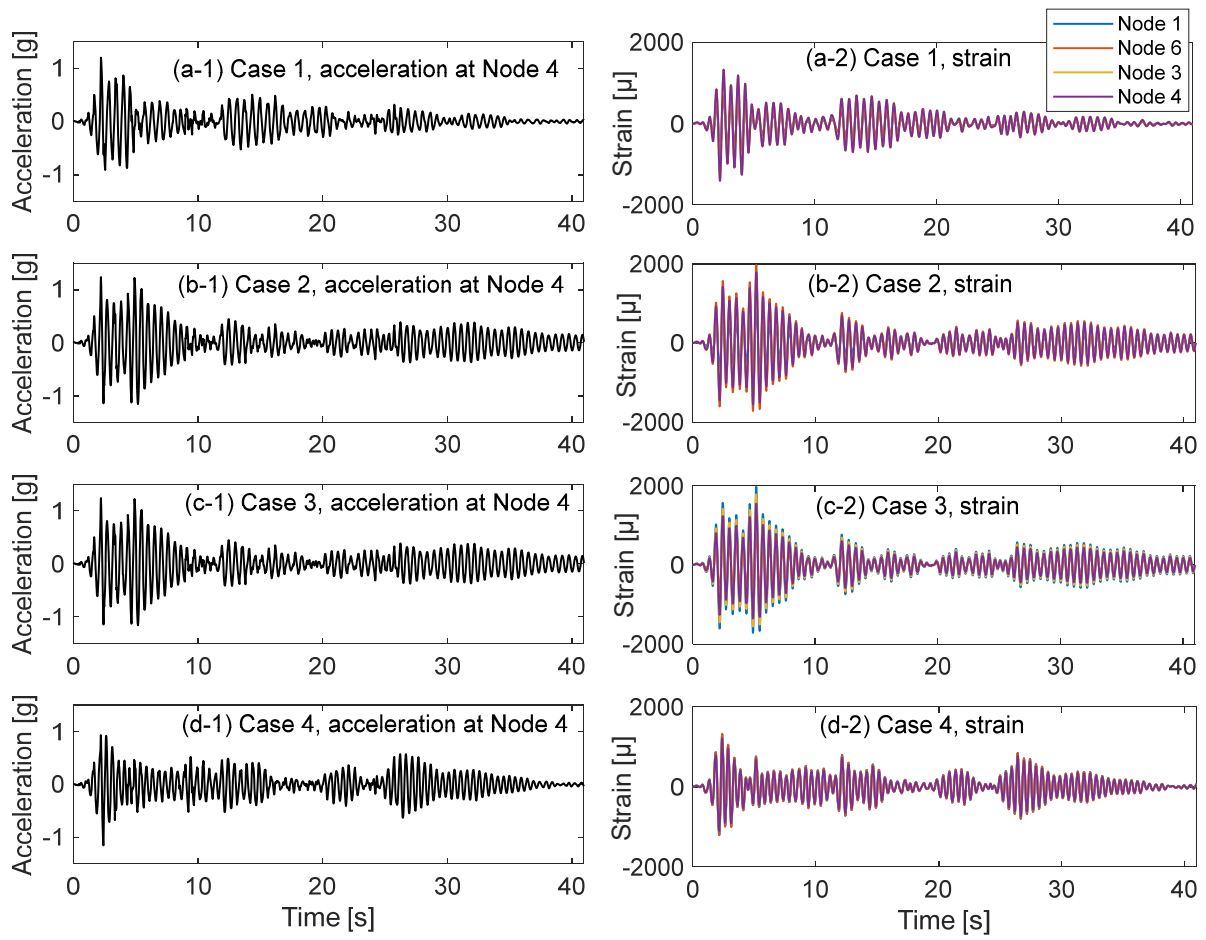


Fig. 6 Time histories of responses in target models

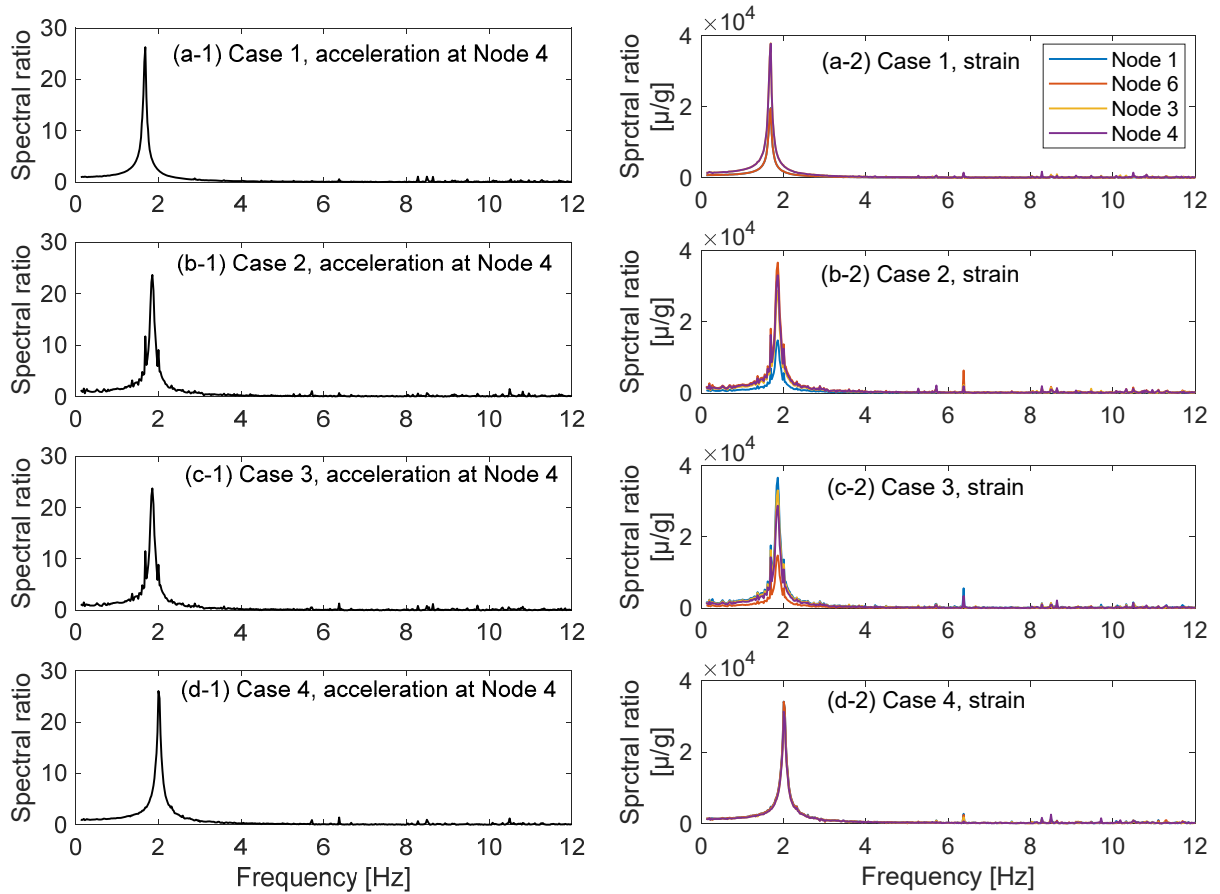


Fig. 7 Fourier amplitude spectral ratios of response to input acceleration for target models

3.3 Training VAE in the space of response analysis model

Response analyses were conducted for various model parameters of the frame structure to construct a dataset to train the VAE. A total of 10^4 pseudo-random numbers for samples of model parameters were generated based on the conditions listed in Table 2. For the input ground motion, the El Centro acceleration time history record from the 1940 Imperial Valley earthquake (north-south component) was used, which was identical to that observed in the target model described in Section 3.2. The acceleration time histories at Node 4, along with dynamic strain time histories at the bottom of Elements 1 and 2, and the top of Elements 3 and 4, were stored as responses corresponding to the target model's observation. Gaussian noise with an S/N ratio of 40 dB, identical to the observed data, was added to both the input and response time histories to stabilize the learning process. Subsequently, the Fourier amplitude spectral ratios of the responses to the input motion were obtained. The logarithm of the Fourier amplitude spectral ratios from 0.1 to 12.6 Hz, i.e., 512 data points, was used as the training dataset. The size of \mathbf{X} is 5×512 .

Diagrams of the encoder, surrogate unimodal encoders and decoder of JMVAE-kl are shown in Fig. 8, 9 and 10, respectively. In this model, the number of dimensions of the latent variables \mathbf{z} is set to 10. The VAE model was trained to minimize the loss function using the Adam optimizer. The training parameters of the VAE are listed in Table 3.

Table 2 Range and probability distribution of parameters for the training dataset

	Ratio of $(EI)_{eq}$ to $(EI)_b$	Stiffness of rotational spring at Node 1 [kNm/rad]	Stiffness of rotational spring at Node 6 [kNm/rad]
Lower bound	1	10	10
Upper bound	10	10^4	10^4
Probability distribution	Uniform distribution in logarithmic axis	Uniform distribution in logarithmic axis	Uniform distribution in logarithmic axis

Table 3 Training parameters for VAE

Batch size	64
Training rate	0.0001
Epoch size	1000

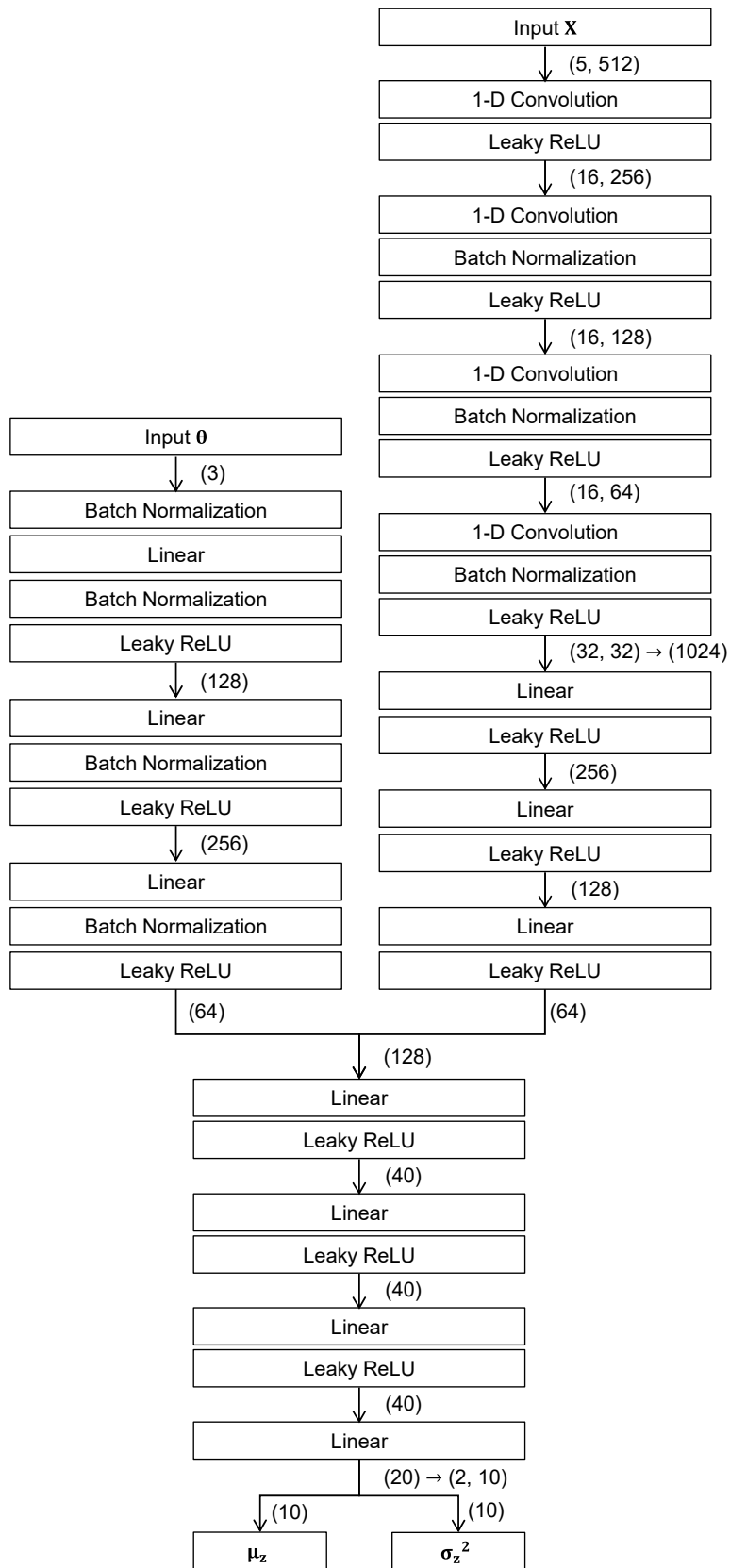
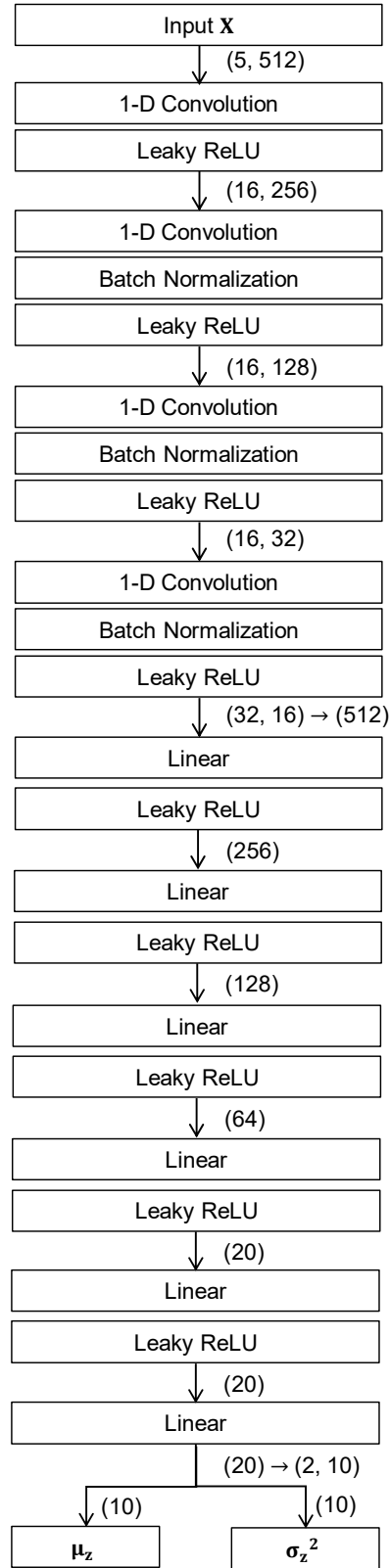
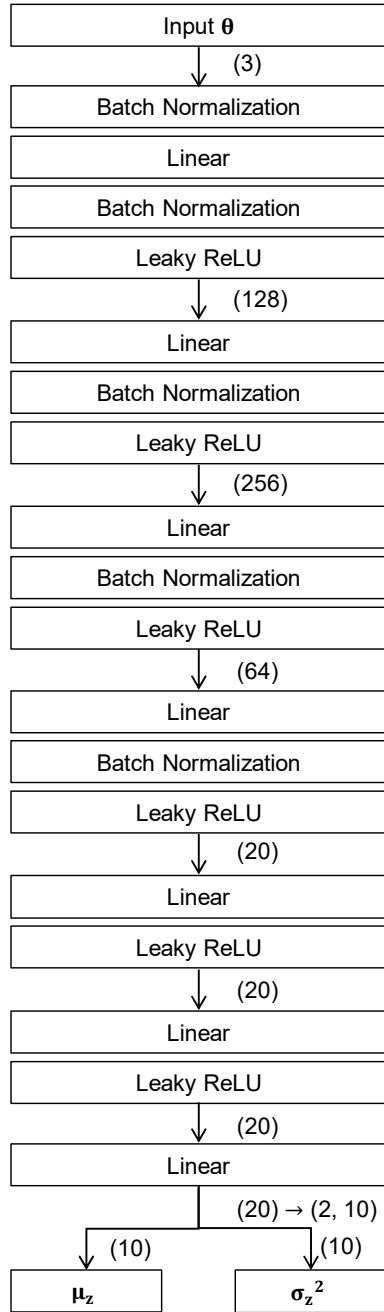


Fig. 8 Diagram of the encoder of JMVAE-kl



(a) Surrogate unimodal model for θ

(b) Surrogate unimodal model for X

Fig. 9 Diagram of the surrogate unimodal encoders of JMVAE-kl

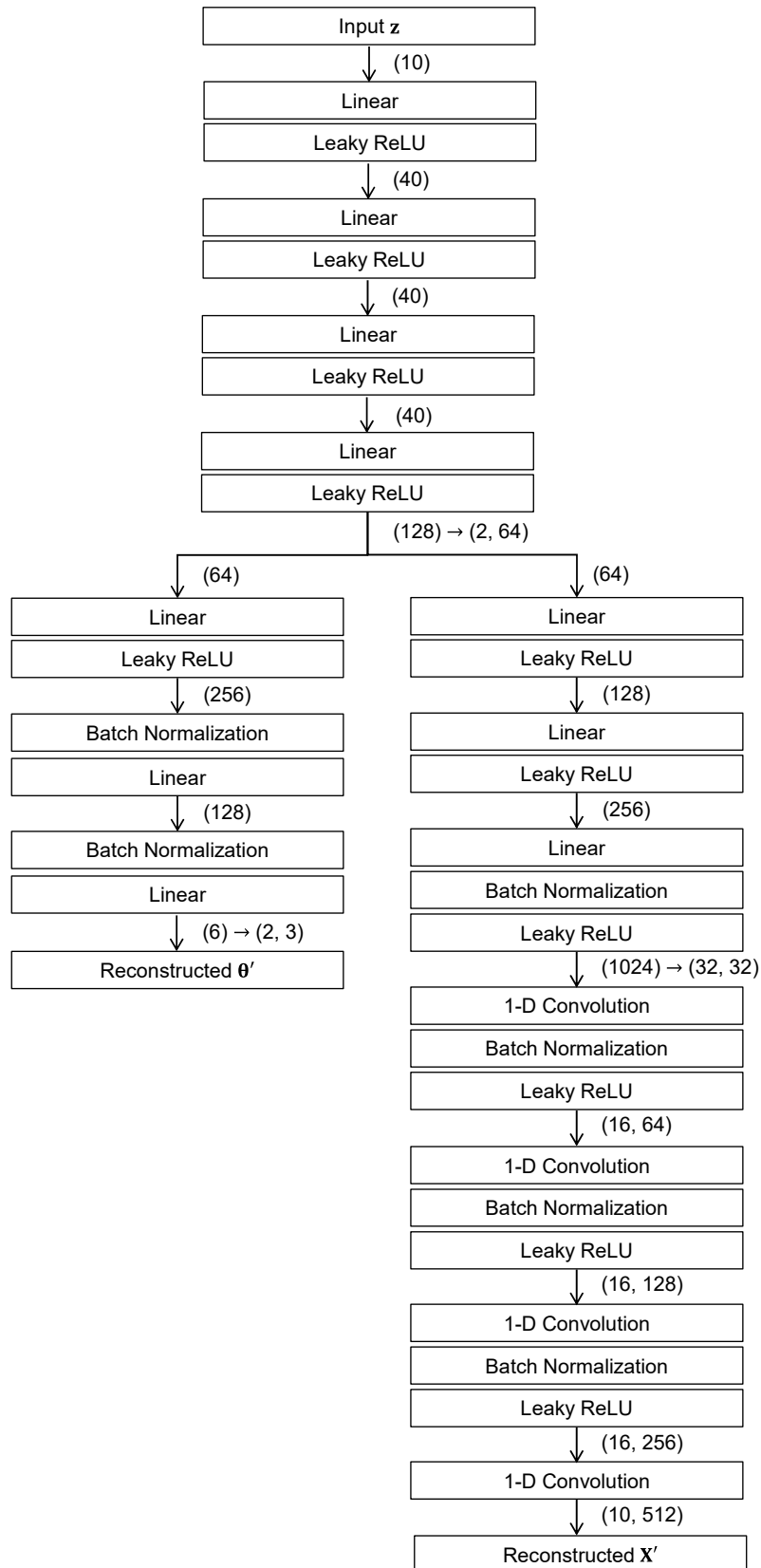


Fig. 10 Diagram of decoder of JMVAE-k1

3.4 Posterior distribution of the model parameters

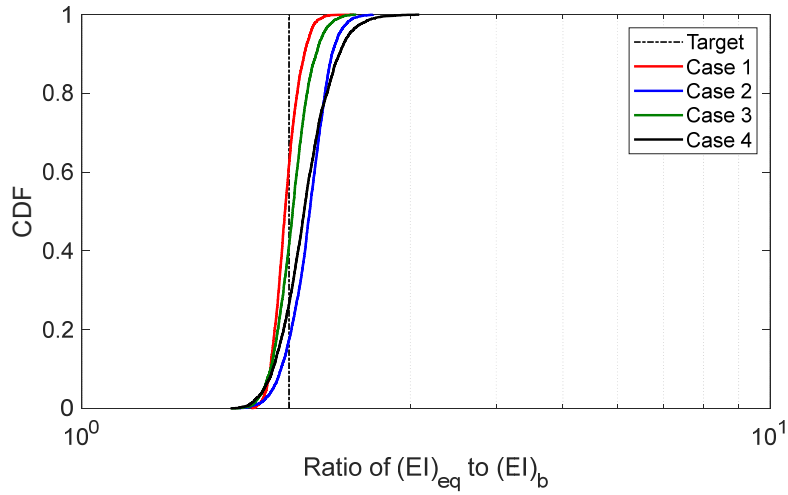
The sampling from the posterior distribution of the model parameters, $p(\boldsymbol{\theta}|\mathbf{X}_{\text{obs}})$, as expressed

in Eq. (8) was performed by the Markov Chain Monte Carlo (MCMC) method with the Metropolis-Hastings algorithm [29], [30]. In this study, a uniform distribution was assumed for the prior distribution $p(\boldsymbol{\theta})$ for simplification. A total of 1000 samples of $\boldsymbol{\theta}$ are obtained. In the MCMC process, the normal distribution is used as the proposal distribution and the standard deviation is set to 0.1 times the parameter range. The first 10000 samples were discarded as the burn-in samples. The samples were then thinned by retaining every 100th sample.

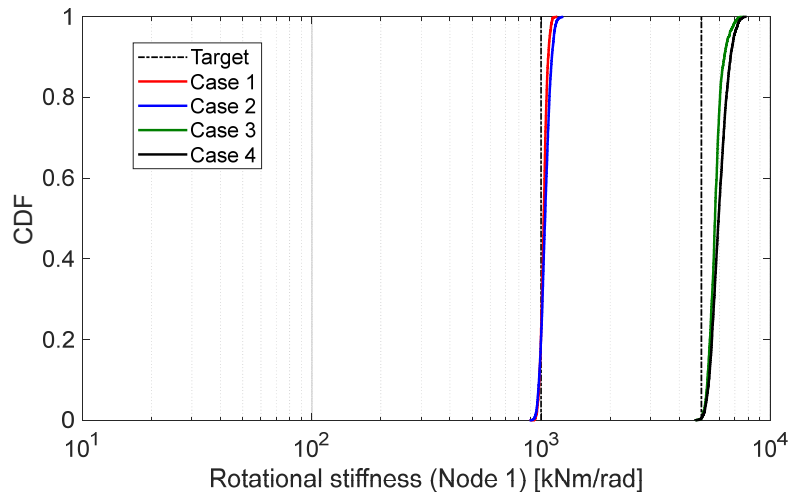
The posterior cumulative distribution function of the updated model parameters $\boldsymbol{\theta}$ obtained using the samples from MCMC are shown in Fig. 11. The estimated model parameters are close to the target values in all four cases. The uncertainty in the estimated model parameters is also presented, with a wider range of $(EI)_{eq}/(EI)_b$ values than those of the rotational stiffnesses. This difference arises because information on the rotational stiffness can be obtained from the strains at the top and bottom of the columns, while the information on $(EI)_{eq}/(EI)_b$ is obtained by combining information on estimated rotational stiffnesses and observed strains. Therefore, the accuracy of $(EI)_{eq}/(EI)_b$ depends on the estimated rotational stiffnesses. Consequently, the uncertainty in $(EI)_{eq}/(EI)_b$ is more significant than those in the rotational stiffnesses.

The proposed Bayesian updating method successfully quantified the uncertainty in the estimated model parameters. The degree of uncertainty depends on whether the observed data include information about the parameters, which in turn could depend on the arrangement and types of measurements, number of measurement points, and characteristics of the observed data. As discussed in Section 3.2, the design and optimization of the measurement and types of data \mathbf{X}_{obs} affect the uncertainty of the estimated model parameters, and optimizing these choices warrants further discussion. The ability to evaluate such an uncertainty is the strength of this method.

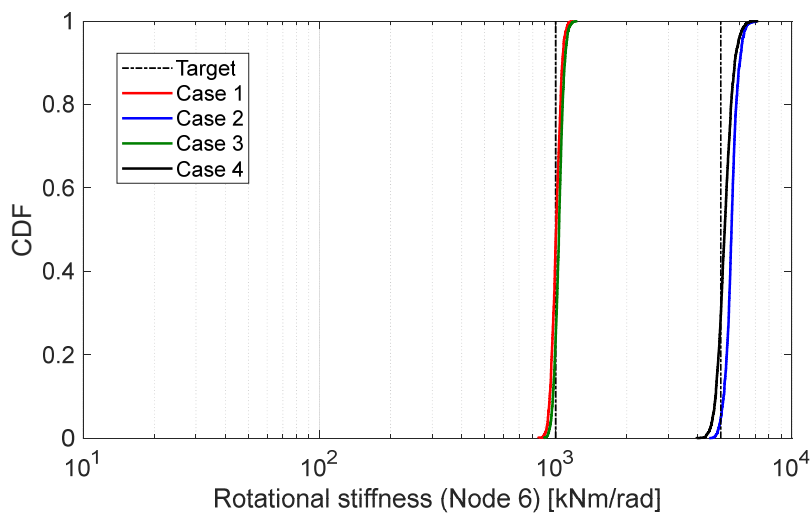
When applying the proposed method to actual structures and observed data, selecting an appropriate model, that is model selection, becomes an additional issue, which will be discussed in future studies.



(a) Ratio of $(EI)_{eq}$ to $(EI)_b$



(b) Rotational stiffness of the rotation spring at Node 1



(c) Rotational stiffness of the rotation spring at Node 6

Fig. 11 Cumulative distribution function of the posterior distribution of model parameters

4. Conclusions

This study proposed a versatile framework for Bayesian structural model updating by employing the surrogate unimodal encoders of JMVAE-kl, a type of multimodal variational autoencoder (VAE). The proposed method is particularly suitable for simultaneous high-dimensional correlated observations used in structural model updating. A numerical example served as a benchmark for the framework, demonstrating updating the model parameters of a single-story frame building structure equipped with acceleration and dynamic strain measurements. The proposed Bayesian updating method successfully quantified the uncertainty in the estimated model parameters. The degree of uncertainty depends on whether the observed data includes information about the parameters. This dependency is influenced by both the arrangement and types of measurements as well as the number of measurement points and the characteristics of the observed data, which will be investigated in future studies.

Data Availability

The data used to support the findings of this study are available from the corresponding author upon reasonable request.

Acknowledgements

Part of this study was supported by the MEXT Innovative Nuclear Research and Development Program [grant number JPMXD0222682433].

References

- [1] Beck, J. L., Katafygiotis, L. S.: Updating Models and Their Uncertainties. I: Bayesian Statistical Framework, *J. Eng. Mech.*, Vol. 124, No. 4, 455-461, 1998.
- [2] Papadimitriou, C., Beck, J. L., Katafygiotis, L.S.: Updating robust reliability using structural test data, *Probabilistic Eng. Mech.*, Volume 16, Issue 2, 103-113, 2001.
- [3] Huang, Y., Shao, C., Wu, B., Beck, J. L., Li, H.: State-of-the-art review on Bayesian inference in structural system identification and damage assessment, *Adv. Struct. Eng.*, Vol. 22, No. 6, 1329-1351, 2019.
- [4] Straub, D., Papaioannou, I.: Bayesian Updating with Structural Reliability Methods, *J. Eng. Mech.*, 141(3), 04014134, 2015.
- [5] Beck, J.L., and Au, S. K.: Bayesian Updating of Structural Models and Reliability using Markov Chain Monte Carlo Simulation, *J. Eng. Mech.*, Vol. 128, No. 4, 380-391, 2002.
- [6] Moehle, J., and Deierlein, G., A Framework Methodology for Performance-Based Earthquake Engineering, *Proceedings, 13th World Conference on Earthquake Engineering*, Vancouver, British Columbia, Paper No. 679, 2004.
- [7] Applied Technology Council: *Seismic Performance Assessment of Buildings, Volume 1 – Methodology*, Second Edition, FEMA P-58-1, 2018.

- [8] Vanik, M. W., Beck, J. L., Au, S. K.: Bayesian Probabilistic approach to structural health monitoring, *J. Eng. Mech.*, 126(7), 738-745, 2000.
- [9] Song, M., Renson, L., Noël, J.-P., Moaveni, B.: Bayesian model updating of nonlinear systems using nonlinear normal modes, *Struct. Control Health Monit.*, 25(12), e2258, 2018.
- [10] Betz, W., Papaioannou, I., Beck, J. M., Straub, D.: Bayesian inference with Subset Simulation: Strategies and improvements, *Computer Methods in Applied Mechanics and Engineering*, Vol. 331, pp. 72-93, 2018.
- [11] Kitahara, M., Dang, C., Beer, M.: Bayesian updating with two-step parallel Bayesian optimization and quadrature, *Computer Methods in Applied Mechanics and Engineering*, Vol. 403, Part A, 115735, 2023.
- [12] Muto, M., Beck, J. L.: Bayesian Updating and Model Class Selection for Hysteretic Structural Models Using Stochastic Simulation, *J. Vib. Control*, Volume 14, Issue 1-2, 7-34, 2008.
- [13] Kitahara, M. Bi, S., Broggi, M., Beer, M.: Bayesian Model Updating in Time Domain with Metamodel-Based Reliability Method, *ASCE ASME J. Risk Uncertain. Eng. Syst. A Civ. Eng., Part A: Civil Engineering*, Vol. 7, No. 3, 04021030, 2021.
- [14] Jerez, D. J., Jensen, H. A., Beer, M.: An effective implementation of reliability methods for Bayesian model updating of structural dynamic models with multiple uncertain parameters, *Reliab. Eng. Syst. Saf.*, Vol. 225, 108634, 2022.
- [15] E. L. Zhang, P. Feissel, J. Antoni, A comprehensive Bayesian approach for model updating and quantification of modeling errors, *Probabilistic Eng. Mech.*, 26, 550–560, 2011.
- [16] E. Zhang, J. D. Chazot, J. Antoni, M. Hamdi, Bayesian characterization of young's modulus of viscoelastic materials in laminated structures, *J. Sound Vib.*, 332, 3654–3666, 2013.
- [17] Song, C., Wang, Z., Shafieezadeh, A., Xiao, R.: BUAK-AIS: Efficient Bayesian Updating with Active learning Kriging-based Adaptive Importance Sampling, *Computer Methods in Applied Mechanics and Engineering*, Vol. 391, 114578, 2022.
- [18] Arangio, S., Beck, J. L.: Bayesian neural networks for bridge integrity assessment, *Struct. Control Health Monit.*, 19(1), 3-21, 2012.
- [19] Ni, P., Li, J., Hao, H., Han, Q., and Du X.: Probabilistic model updating via variational Bayesian inference and adaptive Gaussian process modeling, *Comput. Methods Appl. Mech. Eng.*, Volume 383, 113915, 2021.
- [20] Lee, S., Matsumoto, Y., Yaoyama, T., Hida, T., Itoi, T.: Challenges in Model Identification for Seismic Performance Evaluation of Building Accounting for Uncertainties, 14th International Conference on Applications of Statistics and Probability in Civil Engineering (ICASP14), Dublin, Ireland, 2023.
- [21] Liu, Y., Li, L., Chang, Z.: Efficient Bayesian model updating for dynamic systems, *Reliab. Eng. Syst. Saf.*, Volume 236, 109294, 2023.
- [22] Baltrusaitis, T., Ahuja, C., and Morency, L.-P.: Multimodal machine learning: A survey and taxonomy. *IEEE Trans. Pattern Anal. Mach. Intell.*, 41(2):423–443, 2018.

- [23] Suzuki, M., Nakayama, K., and Matsuo, Y.: Joint multimodal learning with deep generative models, arXiv preprint arXiv:1611.01891, 2016.
- [24] Suzuki, M., Matsuo, Y.: A survey of multimodal deep generative models, *Adv Robot.*, Volume 36, Issue 5-6, 2022.
- [25] Kingma, D. P. and Welling, M.: Auto-encoding variational bayes, Conference proceedings: papers accepted to the International Conference on Learning Representations (ICLR) 2014, 2014.
- [26] McKenna, F. Scott, M. H., Fenves, G. L.: Nonlinear Finite-Element Analysis Software Architecture Using Object Composition, *J. Comput. Civ. Eng.*, 24(1), pp. 95 – 107, 2010.
- [27] Zhu, M., McKenna, F., Scott, M. H.: OpenSeesPy: Python library for the OpenSees finite element framework, *SoftwareX*, 7, pp. 6 – 11, 2018.
- [28] Yaoyama, T., Itoi, T., Iyama, J.: Damage detection and model updating of a steel frame structure by measured strain and acceleration for improving seismic performance assessment, 14th International Conference on Applications of Statistics and Probability in Civil Engineering (ICASP14), Dublin, Ireland, 2023.
- [29] Metropolis, N., Rosenbluth, A.W., Rosenbluth, M.N., Teller, A.H., and Teller, E.: Equation of State Calculations by Fast Computing Machines, *J. Chem. Phys.*, 21(6), 1087–1092, 1953.
- [30] Hasting, W. K.: Monte Carlo Sampling Methods Using Markov Chains and Their Applications, *Biometrika*, Vol. 57, No. 1, 97-109, 1970.